ELSEVIER

Semiempirical and *ab initio* conformational analysis of 2-methylene-8,8-dimethyl-1,4,6,10-tetraoxaspiro[4.5] decane with application of GIAO-SCF methods to NMR spectrum interpretation

C. David Harris,* Andrew J. Holder,* J. David Eick,† Cecil C. Chappelow,‡ and J.W. Stansbury§

**Department of Chemistry, University of Missouri-Kansas City, Kansas City, Missouri, USA*
†School of Dentistry, University of Missouri-Kansas City, Kansas City, Missouri, USA
‡Midwest Research Institute, Kansas City, Missouri, USA
§Dental and Medical Materials/Polymers Division, National Institute of Standards and Technology, Gaithersburg, Maryland, USA

The GIAO-SCF method for calculating isotropic nuclear magnetic shielding values has been utilized to explain certain features in the ^{1}H-NMR spectrum of 2-methylene-8,8-dimethyl-1,4,6,10-tetraoxaspiro[4.5] decane. Population distributions of the low-energy conformers based on their ab initio *energies were used to produce weighting factors for the individual calculated shielding values to calculate the weighted average of the shielding values for a complete set of conformers. The differences in ^{1}H chemical shifts between the hydrogens of the two methyl groups and between the axial and equatorial hydrogens in 2-methylene-8,8-dimethyl-1,4,6,10-tetraoxaspiro[4.5] decane were shown to be due to energy differences between the chair and boat orientations of the six-membered ring and contribution from a twist-boat conformation. Results suggest a hypothesis that intramolecular differences in chemical shift might be calculated to a greater degree of accuracy than chemical shifts calculated relative to a standard.* © *2000 by Elsevier Science Inc.*

Keywords: chemical shift, GIAO-SCF, spiroorthocarbonate, isotropic shielding, nuclear magnetic resonance, conformational population distribution

Corresponding author: C.D. Harris, Department of Chemistry, University of Missouri-Kansas City, 5100 Rockhill Road, Kansas City, MO 64110, USA. Tel.: 816-235-2287; fax: 816-235-5502.

E-mail address: harrisc@cctr.umkc.edu (C.D. Harris)

INTRODUCTION

The synthesis and analysis of 2-methylene-8,8-dimethyl-1,4,6,10-tetraoxaspiro[4.5] decane (**2**, Figure 1) from 2-chloromethyl-8,8-dimethyl-1,4,6,10-tetraoxaspiro[4.5] decane (**1**, Figure 1) has been reported previously by Stansbury.[1] Characterization of **2** by ^{1}H-NMR showed a difference in chemical shift between the axial and equatorial methylene protons at positions 7 and 9 of 0.10 ppm (doublets at 3.73 and 3.83 ppm, J = 11.1 Hz). A difference of 0.10 ppm between the two methyl groups (singlets at 0.99 and 1.09 ppm) at position 8 in **2** also was reported. Neither of these differences was found in the ^{1}H-NMR spectrum of **1**.

The equivalence of the chemical shifts of the sets of methyl protons and the sets of ring protons in **1** was cited as evidence of rapid interconversion of the six-membered ring.[1] The existence of the difference in chemical shift between the sets of axial and equatorial ring protons and the sets of methyl protons in **2** and the fact that the differences for both the ring protons and the outlying methyl groups were an identical 0.10 ppm were interpreted to suggest a significant contribution from a boat conformer (**2e**, Figure 3).[1]

Calculated heats of formation of conformational geometries of **2** optimized using the AM1 semiempirical model[2] are listed in Table 1. These results do not identify any structures similar to the suggested boat conformer as stable conformations, although a different twist-boat structure was found to represent a local minimum. The axial chair conformer (**2aa**, Figure 2) with the six-membered ring in a chair conformation and the double bond of the vinylidine group oriented in an axial position

Journal of Molecular Graphics and Modelling 18, 567–580, 2000

655 Avenue of the Americas, New York, NY 10010

1093-3263/00/$–see front matter
PII S1093-3263(00)00039-5

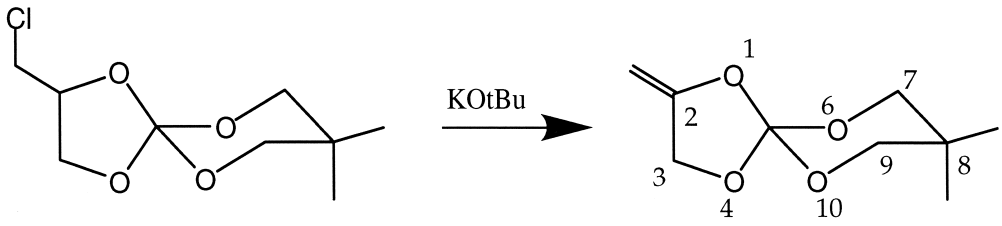

1 **2**

Figure 1. Structures of the chloromethyl precursor, 2-chloromethyl-8,8-dimethyl-1,4,6,10-tetraoxaspiro[4.5] decane **(1)** *and 2-methylene-8,8-dimethyl-1,4,6,10-tetraoxaspiro[4.5] decane* **(2)**.

relative to the six-membered ring was found to be the lowest-energy conformation. The equatorial chair conformation (**2bb**, Figure 2) was calculated to have a heat of formation only 0.29 kcal/mol higher than that of the axial chair. An axial boat conformation that had been proposed as a possible contributor to the spectrum (**2e**, Figure 3) also was used for an initial guess in an AM1 geometry optimization that produced a twist-boat structure (**2cd**, Figure 2) where the methyl carbons are nearly equidistant from the spiro carbon as a local minimum. The heat of formation of **2cd** was calculated to be 0.48 kcal/mol higher in enthalpy than the equatorial chair conformation. The population of this conformer is increased further by the existence of a degenerate enantiomer. Each conformation of **2** optimized using the AM1 model resulted in a planar five-membered ring.

Similar systems containing five- and six-membered rings have been studied using topological methods.[3,4] It was found that in systems containing a five-membered ring joined to a six-membered ring through a spiro carbon, the conformational transformations of the two rings were coupled, and in those compounds with two six-membered rings, the transformations were not coupled. Because the introduction of a double bond into the five-membered ring structure impedes the conformational mobility of the ring, the coupled motions of the six-membered ring may be attenuated further. Hindrance of the mobility of the six-membered ring in this manner may lead to a change in the population distribution of the conformers that result from the motions of the six-membered ring. This might explain the increased difference in chemical shift between the sets of axial and equatorial ring protons and the sets of methyl protons in **2** observed by Stansbury in his NMR experiments.

The purpose of this study is to use semiempirical and *ab initio* molecular orbital calculations to explain these NMR results. Initial review of the available computational methods indicated that the stated errors in calculated chemical shifts are likely too high to adequately describe a difference of only 0.10 ppm.[5–9] However, recent tests of NMR computational methods are limited to ^{13}C and other heavy atoms. Because ^{1}H chemical shifts are reported on a much smaller scale than are those for heavier atoms, we proceeded on the basis that the errors for calculated ^{1}H chemical shifts might be correspondingly lower. There was support in the literature for this in that Ditchfield[10] reported errors for ^{1}H chemical shifts calculated at the 4-31g Hartree-Fock level of theory to be one order of magnitude lower than ^{13}C errors at the same level of theory. Further, using

Table 1. Characterization of geometries: AM1 results

Conformer		AM1 characterization[a]	AM1 heat of formation (kcal/mol)	AM1 difference in heats of formation (kcal/mol)
2aa	Axial chair[b]	Minimum	−168.25	0.29
2bb	Equatorial chair[b]	Minimum	−167.96	
2a	Axial chair[c]	Not critical point		
2a	Axial chair	Not critical point		0.48
2b	Equatorial chair[c]	Not critical point		
2b	Equatorial chair	Not critical point		
2cd	Twist[b,c]	Minimum	−167.48	
2cd	Twist[b,c]	Minimum	−167.48	
2e	Axial boat[c]	Not critical point		
2e	Axial boat	Not critical point		
2f	Equatorial boat[c]	Not critical point		
2f	Equatorial boat	Not critical point		

[a] "Minimum" identifies a local minimum on the potential energy surface; "not critical point" indicates a geometry that is not a stationary point on the potential energy surfaces.
[b] Five-membered ring has a planar geometry.
[c] Conformers are listed twice to account for degenerate isomers.

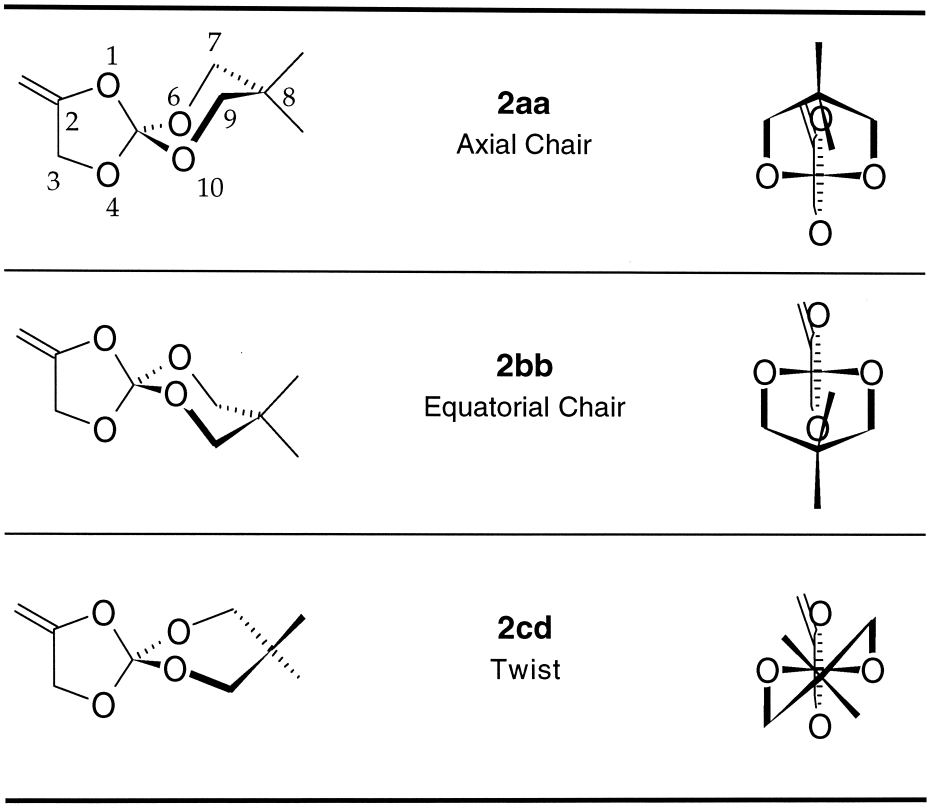

Figure 2. Structures of the conformational isomers of 2-methylene-8,8-dimethyl-1,4,6,10-tetraoxaspiro[4.5] decane identified by AM1 semiempirical calculations.

larger basis sets, Vaara and coworkers[11] reported errors for ^{1}H chemical shifts consistently less than 1 ppm and sometimes less than 0.10 ppm.

In addition, all of the reported chemical shifts were calculated relative to a standard such as tetramethylsilane or methane. Comparison of calculated properties of molecules with different numbers and identities of atoms as well as differences in the number of basis functions used is another source of error in the calculation of chemical shifts. We proceeded with our work using the assumption that comparison of the calculated values of the magnetic shielding for two hydrogen atoms in the same molecule produced by the same calculation should eliminate or greatly reduce this type of systematic error.

CALCULATIONS

Nuclear magnetic shielding value calculations were performed at the HF/6-311+g(2d,p) level of theory using the GIAO-SCF

Table 2. Relative energies of conformers identified as local minima (kcal/mol)

	Conformer								
Method	**2a**	**2aa**	**2b**	**2bb**	**2c**	**2d**	**2cd**	**2e**	**2f**
AM1		0.00		0.29			0.77		
3-21g	0.000		0.610					3.413	3.747
6-311+g(2d,p)//3-21g	0.000		0.554					3.884	4.211
6-31+g(d,p)	0.000		0.367		1.488	1.279			
6-311+g(2d,p)//6-31+g(d,p)	0.000		0.354		1.482	1.653			

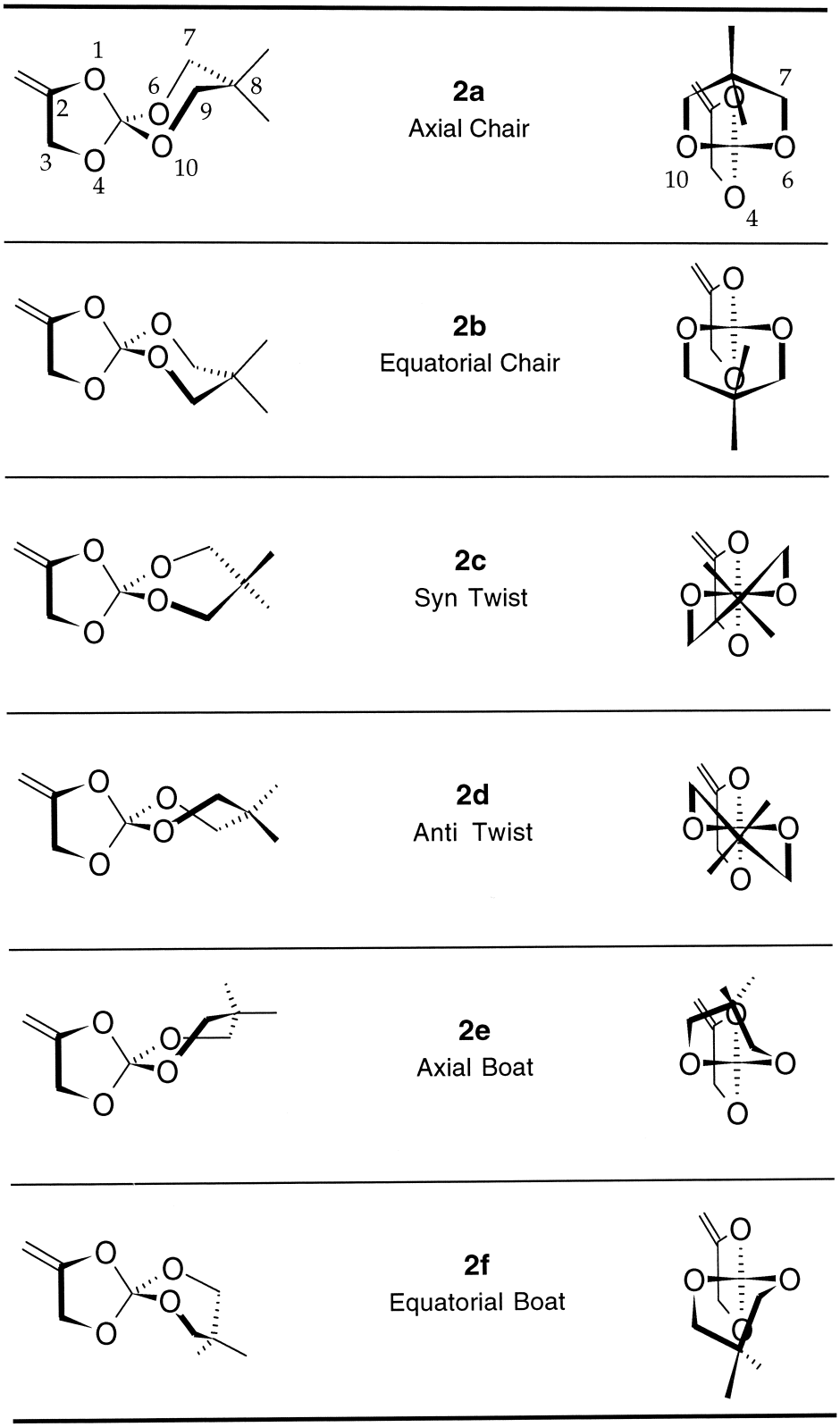

Figure 3. Structures of the conformational isomers of 2-methylene-8,8-dimethyl-1,4,6,10-tetraoxaspiro[4.5] decane identified by ab initio *Hartree-Fock calculations.*

method[10] as implemented in the *Gaussian 94* suite of computational tools[12] on the HF/6-31+g(d,p) optimized geometry of **2a.** Averaging the calculated shielding values for the hydrogens of each methyl group produced a difference in the chemical shifts between the methyl groups of 0.5411 ppm. Although the difference in this result and the observed value of 0.10 ppm is similar to reported errors for calculated chemical shifts, it does not indicate the reduction in error that might be anticipated for intramolecular differences in chemical shifts. Because of these results, plus the enthalpy differences and populations suggested by the AM1 results, it was hypothesized that inclusion of other low-energy conformers might improve the calculation of chemical shift differences. This proved to be the case.

Geometry optimizations were performed for all the low-energy conformations at the RHF/3-21g and RHF/6-31+g(d,p) levels of theory. The resulting geometries were characterized at the same levels of theory by performing frequency calculations. Geometries whose frequency calculations produced no imaginary frequencies were taken to represent local minima on the conformational potential energy surface. Corrections to the Gibbs free energy at 298.15 K were calculated to describe the conformational equilibrium. The relative energies of all conformers that were identified as local minima are shown in Table 2.

The Boltzmann distributions (d_i) of the conformers relative to the lowest-energy conformer were computed using the relationship:

$$d_i = e^{-(E_i - E_0)/kT}. \tag{1}$$

The result then is divided by the total partition function to yield the probability distribution coefficient (c_i) for each conformer:

$$c_i = \frac{e^{-(E_i - E_0)/kT}}{\sum_i e^{-(E_i - E_0)/kT}} = \frac{d_i}{\sum_i d}. \tag{2}$$

These probability distribution coefficients were used as weighting factors for the individual magnetic shielding values calculated for each conformer. Finally, a weighted average for each ring proton and each methyl group proton was calculated based on the sum of the chemical shift values for each conformer weighted by the distribution coefficient (c_i):

$$\delta_{\text{proton}} = \sum_1^i c_i \cdot \delta_{\text{proton},i}. \tag{3}$$

The resulting differences then are compared to experimental results.

RESULTS AND DISCUSSION

RHF/3-21g Geometries

Results from the 3-21g geometry optimizations of **2** and their characterizations are summarized in Table 3. It is useful to define the primary plane of symmetry for this molecule to provide a spatial reference when describing the structures of its conformers. Atoms 1, 4, 5, and 8 (the two oxygens on the five-membered ring, the spiro carbon, and the methyl-substituted carbon) are coplanar in all of the studied conformations. In those conformations containing a planar five-membered ring, the atoms of that ring and the vinylidine protons also inhabit the plane, as well as the methyl carbons in the chair conformers. Graphical representations of the optimized geometries for **2a** and **2b** are shown in Figure 4, along with the numbering system used for the hydrogens of interest to this study. The orientations of the methyl groups represented in Figure 4 indicate the only rotational isomers for which a local energy minimum could be identified. This was the case for all conformers at each level of theory.

Unlike the AM1 results, 3-21g calculations characterize the chair conformers with planar five-membered rings as transition

Table 3. Characterization of geometries and thermal corrections to energies: 3-21g optimized geometries

Conformer		3-21g characterization	3-21g energy (hartrees)	3-21g thermal correction (hartrees)
2aa	Axial chair	Transition state	−644.810805	0.254290
2bb	Equatorial chair	Transition state	−644.809936	0.254281
2a	Axial chair	Minimum	−644.811010	0.255275
2a	Axial chair	Minimum	−644.811010	0.255275
2b	Equatorial chair	Minimum	−644.810013	0.255250
2b	Equatorial chair	Minimum	−644.810013	0.255250
2c	Syn-twist	Not critical point		
2c	Syn-twist	Not critical point		
2d	Anti-twist	Not critical point		
2d	Anti-twist	Not critical point		
2e	Axial boat	Minimum	−644.805563	0.255270
2e	Axial boat	Minimum	−644.805563	0.255270
2f	Equatorial boat	Minimum	−644.805008	0.255248
2f	Equatorial boat	Minimum	−644.805008	0.255248

"Minimum" identifies a local minimum on the potential energy surface; "not critical point" indicates a geometry that is not a stationary point on the potential energy surface; "transition state" indicates a geometry with a single imaginary frequency.

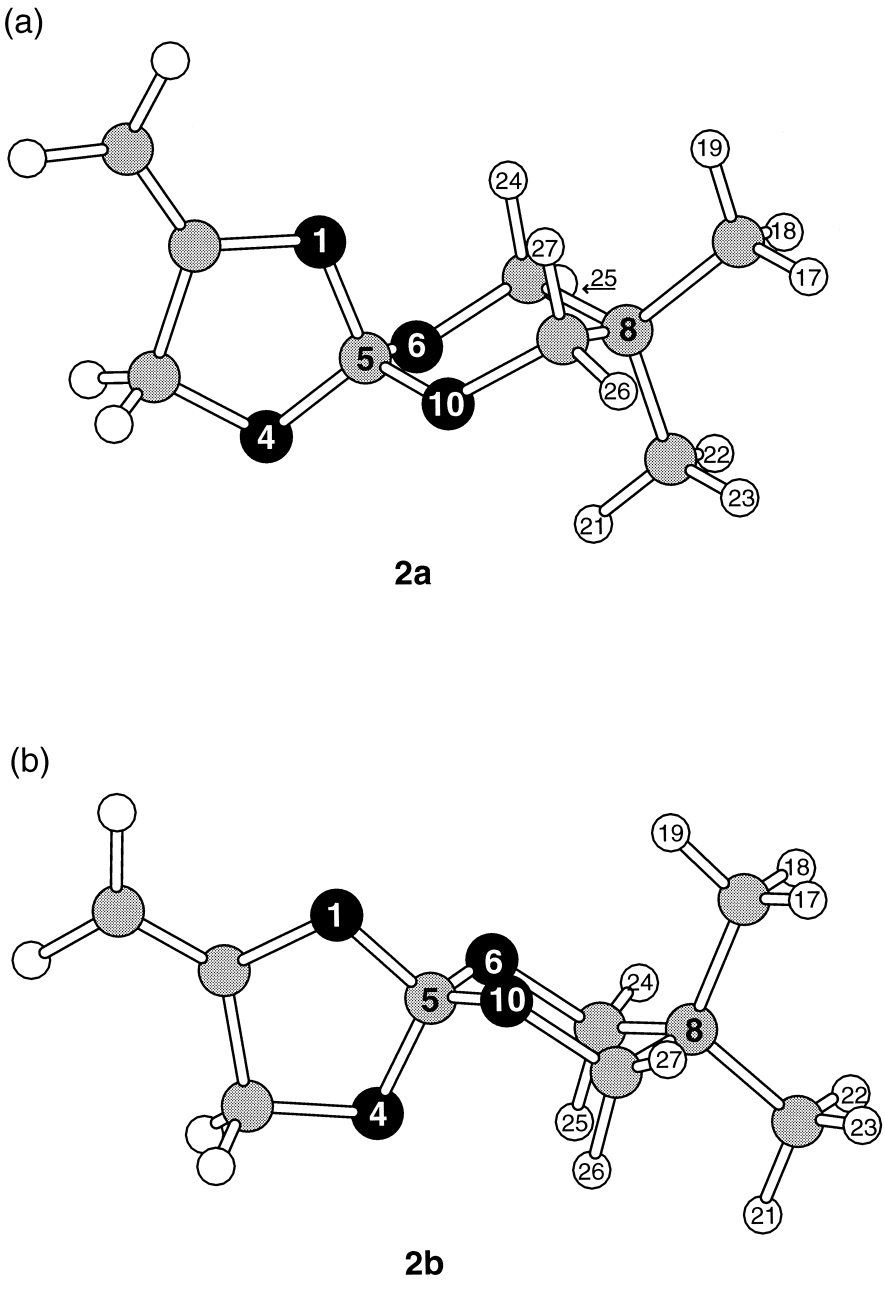

Figure 4. Ball-and-stick representations of the optimized geometries for (a) **2a** *and (b)* **2b**. *The six-membered rings are symmetric with respect to the plane defined by atoms 1, 4, 5, and 8. In both conformers, the five-membered ring is bent away from the viewer in one conformation and bent toward the viewer in its degenerate enantiomer. There are transition states between the enantiomers in which the five-membered rings are planar with the vinylidine group within the plane of symmetry (***2aa** *and* **2bb**). *The hydrogens are numbered according to their input file identifiers, which are unique to this study.*

states. The relative minima that are linked by this transition are two degenerate enantiomers whose five-membered rings are distorted out of the plane of symmetry (**2a**, **2b**). Also in contrast to the AM1 results, the twist-boat structure is not a stationary point on the 3-21g surface. The proposed axial boat structure (**2e**) is a local minimum at the 3-21g level, as is an equatorial boat structure (**2f**). The lowest energy structures are the axial chair conformers, followed by the equatorial chair conformers. The difference in the two is 0.0009722 hartrees (0.6101 kcal/mol). The axial boat conformer is the next highest in energy, 0.0044496 hartrees (2.792 kcal/mol) higher than the equatorial chair. The equatorial boat represents the highest energy local minimum studied, 0.0005471 hartrees (0.3481 kcal/mol) higher than the axial boat.

Calculations of the Boltzmann distribution at the HF/3-21g//HF/3-21g level and the resulting weighting factors are detailed in Table 4. The chair conformations were calculated to have populations of the same order of magnitude, suggesting significant contributions to the NMR spectrum. The boat conformations have calculated populations only a hundredth of those of the chair conformers, and thus their contributions to the calculated spectrum are expected to be much lower than those of the chair conformers.

The 3-21g thermal corrections to the 6-311+g(2d,p) energies calculated for the 3-21g geometries are shown in Table 5. The differences in the 6-311+g(2d,p) energies are similar to those found with the 3-21g energies. The Boltzmann distributions and weighting factors for the 6-311+g(2d,p) energy calculations are shown in Table 6 for all of the 3-21g optimized conformers. The weighting factors for the two boat structures are lower than those for the chair conformers by a factor of

Table 4. Conformational analysis and calculation of distribution coefficients: 3-21g results

	Conformer	Energy (hartrees)	Energy (J)	Boltzmann distribution (d_i) $[e^{-(E_i-E_0)/kT}]$	Distribution coefficient (c_i) $[e^{-(E_i-E_0)/kT}/\sum_i e^{-(E_i-E_0)/kT}]$
2aa	Axial chair	Transition state			Transition state
2bb	Equatorial chair	Transition state			Transition state
2a	Axial chair	−644.555735	−2.810102E-15	1.000000E+00	3.670617E-01
2a	Axial chair	−644.555735	−2.810102E-15	1.000000E+00	3.670617E-01
2b	Equatorial chair	−644.554763	−2.810098E-15	3.572348E-01	1.311272E-01
2b	Equatorial chair	−644.554763	−2.810098E-15	3.572348E-01	1.311272E-01
2c	Syn-twist	Not critical point			Not critical point
2c	Syn-twist	Not critical point			Not critical point
2d	Anti-twist	Not critical point			Not critical point
2d	Anti-twist	Not critical point			Not critical point
2e	Axial boat	−644.550293	−2.810078E-15	3.144875E-03	1.154363E-03
2e	Axial boat	−644.550293	−2.810078E-15	3.144875E-03	1.154363E-03
2f	Equatorial boat	−644.549760	−2.810076E-15	1.789109E-03	6.567135E-04
2f	Equatorial boat	−644.549760	−2.810076E-15	1.789109E-03	6.567135E-04

10^{-3}, indicating that they do not make a significant contribution to the calculated ^{1}H-NMR spectrum.

Calculation of the NMR isotropic shielding values of the 3-21g optimized structures were performed at the RHF/6-311+g(2d,p) level of theory. The results for the ring protons are shown in Table 7 and those for the methyl groups are shown in Table 8. As expected, the boat conformers do not make a significant contribution to the calculated ^{1}H-NMR spectrum. The calculated difference in the chemical shifts of the ring methylene protons is 0.2512 ppm, which differs from the observed value by 0.15 ppm. The calculated difference in the chemical shifts of the methyl groups is 0.2625 ppm, which differs from the experimentally observed value by 0.16 ppm. When the RHF/6-311+g(2d,p) energies are used for the calculation of the distributions, the ring methylene protons differ by 0.2311 ppm and the methyl protons by 0.2417 ppm. These represent a difference from observed values of 0.13 and 0.14 ppm, respectively, indicating improvement in chemical shift calculations with more accurate energies.

RHF/6-31+g(d,p) Geometries

Geometry optimizations at the 6-31+g(d,p) level of theory of the chair conformers confirm the 3-21g results and are summarized in Table 9. Thermal corrections to the Gibbs free energy are shown in Table 9 for 6-31+g(d,p) energies and in Table 11 for 6-311+g(2d,p)//6-31+g(d,p) energies. The chair conformers with planar five-membered rings are transition states between degenerate enantiomers, as in the 3-21g results. In contrast to the 3-21g results, the boat conformers were not stationary points on the potential energy surface. Instead, two twist-boat structures (each with a degenerate enantiomer with

Table 5. Characterization of geometries and thermal corrections to energies: 3-21g optimized geometries

	Conformer	3-21g characterization	6-311+g(2d,p) energy (hartrees)	3-21g thermal correction (hartrees)	6-311+g(2d,p) corrected energy (hartrees)
2aa	Axial chair	Transition state		0.254290	Transition state
2bb	Equatorial chair	Transition state		0.254281	Transition state
2a	Axial chair	Minimum	−648.574716	0.255275	−648.319441
2a	Axial chair	Minimum	−648.574716	0.255275	−648.319441
2b	Equatorial chair	Minimum	−648.573808	0.255250	−648.318558
2b	Equatorial chair	Minimum	−648.573808	0.255250	−648.318558
2c	Syn-twist	Not critical point			Not critical point
2c	Syn-twist	Not critical point			Not critical point
2d	Anti-twist	Not critical point			Not critical point
2d	Anti-twist	Not critical point			Not critical point
2e	Axial boat	Minimum	−648.568517	0.255270	−648.313247
2e	Axial boat	Minimum	−648.568517	0.255270	−648.313247
2f	Equatorial boat	Minimum	−648.567973	0.255248	−648.312725
2f	Equatorial boat	Minimum	−648.567973	0.255248	−648.312725

Table 6. Conformational analysis and calculation of distribution coefficients: 6-311+g(2d,p)//3-21g results

Conformer		Energy (hartrees)	Energy (J)	Boltzmann distribution (d_i) [$e^{-(E_i-E_0)/kT}$]	Distribution coefficient (c_i) [$e^{-(E_i-E_0)/kT}/\sum_i e^{-(E_i-E_0)/kT}$]
2aa	Axial chair	Transition state			Transition state
2bb	Equatorial chair	Transition state			Transition state
2a	Axial chair	−648.319441	−2.826511E-15	1.000000E+00	3.584840E-01
2a	Axial chair	−648.319441	−2.826511E-15	1.000000E+00	3.584840E-01
2b	Equatorial chair	−648.318558	−2.826507E-15	3.925282E-01	1.407151E-01
2b	Equatorial chair	−648.318558	−2.826507E-15	3.925282E-01	1.407151E-01
2c	Syn-twist	Not critical point			Not critical point
2c	Syn-twist	Not critical point			Not critical point
2d	Anti-twist	Not critical point			Not critical point
2d	Anti-twist	Not critical point			Not critical point
2e	Axial boat	−648.313247	−2.826484E-15	1.417738E-03	5.082365E-04
2e	Axial boat	−648.313247	−2.826484E-15	1.417738E-03	5.082365E-04
2f	Equatorial boat	−648.312725	−2.826481E-15	8.163303E-04	2.926414E-04
2f	Equatorial boat	−648.312725	−2.826481E-15	8.163303E-04	2.926414E-04

respect to the previously described plane of symmetry) were identified as local minima. These conformers are similar to the twist-boat structure produced by AM1 calculations, but with a nonplanar five-membered ring. To assist in the description of the twist-boat geometries, we introduce a second plane of reference that is defined by atoms 5, 6, and 10 (the spiro carbon and the two oxygens of the six-membered ring). Extension of the two planes divides space into four quadrants (Figure 5). The twist-boat structure in which the methylene group of the double bond occupies the same quadrant as a methyl group on the six-membered ring is the "syn-twist" conformer (**2c**). The twist-boat structure whose exo-methylene group is in a quadrant without a methyl group is the "anti-twist" conformer (**2d**). It is presumed that transition states exist with near-planar five-membered rings that link one syn-twist conformer with one anti-twist conformer, but these transition states have not been identified computationally.

As in the 3-21g results, the lowest energy structures are the

Table 7. Calculated magnetic shielding tensors for methylene protons on six-membered ring: 3-21g geometries and 6-311+g(2d,p) energies

Conformer	Distribution coefficient	Calculated magnetic shielding tensors for ring methylene proton				Weighted magnetic shielding tensors for ring methylene proton			
		24	25	26	27	24	25	26	27
2aa	Transition state								
2bb	Transition state								
2a	0.358484	28.6382	29.1820	29.2650	28.7311	10.2663	10.4613	10.4910	10.2996
2a	0.358484	28.7311	29.2650	29.1820	28.6382	10.2996	10.4910	10.4613	10.2663
2b	0.140715	29.2123	28.6558	28.7209	29.2702	4.1106	4.0323	4.0415	4.1188
2b	0.140715	29.2702	28.7209	28.6568	29.2123	4.1188	4.0415	4.0324	4.1106
2c	Not critical point								
2c	Not critical point								
2d	Not critical point								
2d	Not critical point								
2e	0.000508	28.9057	29.1459	28.8031	29.3013	0.0147	0.0148	0.0146	0.0149
2e	0.000508	29.3013	28.8031	29.1459	28.9057	0.0149	0.0146	0.0148	0.0147
2f	0.000293	28.7863	29.3198	29.9268	29.1455	0.0084	0.0086	0.0088	0.0085
2f	0.000293	29.1455	29.9268	29.3198	28.7863	0.0085	0.0088	0.0086	0.0084
			Weighted average			28.8419	29.0729	29.0730	28.8419
			Calculated average difference			0.2311 ppm			
			Experimental difference			0.1000 ppm			

Table 8. Calculated magnetic shielding tensors for protons on methyl substituents: 3-21g geometries and 6-311+g(2d,p) energies

Conformer	Distribution coefficient	Calculated magnetic shielding tensors for methyl group 1				Calculated magnetic shielding tensors for methyl group 2				Weighted averages	
		17	18	19	Average	21	22	23	Average	Methyl 1	Methyl 2
2aa	Transition state										
2bb	Transition state										
2a	0.358484	31.7398	31.7406	31.9225	31.8010	30.1611	31.7602	31.7648	31.2287	11.4001	11.1950
2a	0.358484	31.7406	31.7398	31.9225	31.8010	30.1611	31.7648	31.7602	31.2287	11.4001	11.1950
2b	0.140715	31.7640	31.7655	30.1366	31.2220	31.9537	31.7530	31.7536	31.8201	4.3934	4.4776
2b	0.140715	31.7655	31.7640	30.1366	31.2220	31.9537	31.7536	31.7530	31.8201	4.3934	4.4776
2c	Not critical point										
2c	Not critical point										
2d	Not critical point										
2d	Not critical point										
2e	0.000508	31.8198	31.7074	30.0212	31.1828	31.6651	31.5131	31.8179	31.6654	0.0158	0.0161
2e	0.000508	31.7074	31.8198	30.0212	31.1828	31.6651	31.8179	31.5131	31.6654	0.0158	0.0161
2f	0.000293	31.5269	31.8252	31.6606	31.6709	30.1000	31.8445	31.7591	31.2345	0.0093	0.0091
2f	0.000293	31.5269	31.6606	31.8252	31.6709	31.1000	31.7591	31.8445	31.5679	0.0093	0.0092
						Weighted average				31.6373	31.3957
						Calculated average difference				0.2417 ppm	
						Experimental difference				0.1000 ppm	

axial chair conformers, followed by the equatorial chair conformers. The difference in the two is 0.0005779 hartrees (0.3626 kcal/mol). The syn-twist conformer is the next highest in energy, 0.0022384 hartrees (1.405 kcal/mol) higher than the equatorial chair. The anti-twist represents the highest energy local minimum studied at the 6-31+g(d,p) level, 0.0002146 hartrees (0.1347 kcal/mol) higher than that of the syn-twist conformer. The four energy levels of the 6-31+g(d,p) optimized conformers are closer together than those of the 3-21g optimized conformers. The 6-31+g(d,p) energies are distributed over a range of 1.9023 kcal/mol and the 3-21g energies are distributed over a range of 3.7502 kcal/mol. This suggests that the 6-31+g(d,p) optimized conformers have a more significant effect on the calculated spectrum than do the higher-energy conformers from the 3-21g optimizations.

Calculations of the Boltzmann distribution and weighting factors are detailed in Table 10 for the 6-31+g(d,p)//6-31+g(d,p) energies and in Table 12 for the 6-311+g(2d,p)//6-

Table 9. Characterization of geometries and thermal corrections to energies: 6-31+g(d,p) optimized geometries

Conformer		6-31g+(d,p) characterization	6-31g+(d,p) energy (hartrees)	6-31g+(d,p) thermal correction (hartrees)	6-31g+(d,p) corrected energy (hartrees)
2aa	Axial chair	Transition state	−648.427871	0.205709	Transition state
2bb	Equatorial chair	Transition state	−648.427315	0.205934	Transition state
2a	Axial chair	Minimum	−648.428773	0.206272	−648.222501
2a	Axial chair	Minimum	−648.428773	0.206272	−648.222501
2b	Equatorial chair	Minimum	−648.428195	0.206279	−648.221916
2b	Equatorial chair	Minimum	−648.428195	0.206279	−648.221916
2c	Syn-twist	Minimum	−648.425957	0.205829	−648.220128
2c	Syn-twist	Minimum	−648.425957	0.205829	−648.220128
2d	Anti-twist	Minimum	−648.425742	0.205281	−648.220461
2d	Anti-twist	Minimum	−648.425742	0.205281	−648.220461
2e	Axial boat	Not critical point			Not critical point
2e	Axial boat	Not critical point			Not critical point
2f	Equatorial boat	Not critical point			Not critical point
2f	Equatorial boat	Not critical point			Not critical point

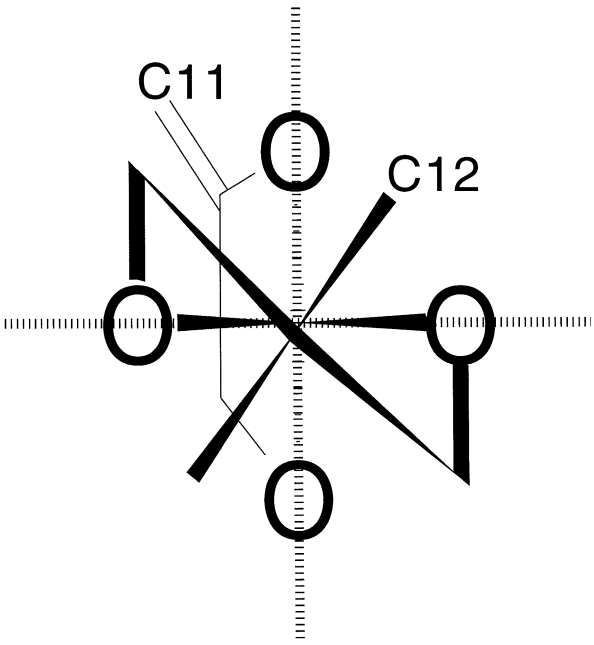

*Figure 5. Illustration of criterion for assignment of "anti" or "syn" designation to the twist conformers of 2-methylene-8,8-dimethyl-1,4,6,10-tetraoxaspiro[4.5] decane. Broken lines indicate planes that pass through the spiro carbon and the oxygens of a ring. The orthogonal planes divide space into four quadrants. The twist conformer with C11 and C12 in different quadrants (***2d***, shown) is the anti-twist conformer. The syn-twist conformer (***2c***) has C11 and C12 in the same quadrant.*

31+g(d,p) energies. Like the 3-21g structures, the higher-level energy calculations make little difference in the distribution of conformers. As expected, the weighting factors are less widely spaced than those calculated for the 3-21g conformers. The values for the weighting factors differ only by a factor of 10, suggesting that they are all significant contributors to the calculated spectrum.

Calculations of the magnetic shielding values, their weighted averages, and the difference in chemical shifts of the ring methylene protons are shown in Table 13. The calculated difference in chemical shifts between the ring methylene protons is 0.1107 ppm. This differs from the observed value by 0.01 ppm, which is below previously reported errors for calculated chemical shifts relative to a standard.

Corresponding calculations for the methyl groups are summarized in Table 14. The calculated difference in chemical shifts between the two methyl groups is 0.1326 ppm, which differs from the observed value by 0.03 ppm and is greater than the error reported for the ring methylene protons but still lower than previously reported errors in calculated chemical shifts relative to a standard. These calculations are based on the weighting factors calculated using the 6-31+g(d,p)//6-31+g(d,p) energies.

Calculations based on the weighting factors using the 6-311+g(2d,p)//6-31+g(d,p) energies are shown in Table 15 for the methylene protons and in Table 16 for the methyl groups. These results show a difference in chemical shift between the ring methylene protons of 0.1104 ppm. The difference in calculated chemical shift between the methyl groups was 0.1331 ppm.

CONCLUSIONS

Calculated NMR parameters can be used to elucidate unexplained or ambiguous results from experimental measurements. The results of this study are consistent with a sample that undergoes rapid conformational changes. Because of the asymmetry of the five-membered ring, the two chair conformers are unequal in energy and population. This population difference is responsible for the differences in chemical shift between the axial and equatorial ring methylene protons and between the protons of the two methyl groups in **2** that were not observed in **1**. The boat structures of **2e** and **2f** were found not to be contributors to the calculated ^{1}H-NMR spectrum. The twist

Table 10. Conformational analysis and calculation of distribution coefficients: 6-31+g(d,p) results

	Conformer	Energy (hartrees)	Energy (J)	Boltzmann distribution (d_i) $[e^{-(E_i-E_0)/kT}]$	Distribution coefficient c_i) $[e^{-(E_i-E_0)/kT}/\sum_i e^{-(E_i-E_0)/kT}]$
2aa	Axial chair	Transition state			Transition state
2bb	Equatorial chair	Transition state			Transition state
2a	Axial chair	−648.222501	−2.826088E-15	1.000000E+00	2.882320E-01
2a	Axial chair	−648.222501	−2.826088E-15	1.000000E+00	2.882320E-01
2b	Equatorial chair	−648.221916	−2.826085E-15	5.383363E-01	1.551658E-01
2b	Equatorial chair	−648.221916	−2.826085E-15	5.383363E-01	1.551658E-01
2c	Syn-twist	−648.220128	−2.826078E-15	8.103560E-02	2.335706E-02
2c	Syn-twist	−648.220128	−2.826078E-15	8.103560E-02	2.335706E-02
2d	Anti-twist	−648.220461	−2.826079E-15	1.153415E-01	3.324512E-02
2d	Anti-twist	−648.220461	−2.826079E-15	1.153415E-01	3.324512E-02
2e	Axial boat	Not critical point			Not critical point
2e	Axial boat	Not critical point			Not critical point
2f	Equatorial boat	Not critical point			Not critical point
2f	Equatorial boat	Not critical point			Not critical point

Table 11. Characterization of geometries and thermal corrections to energies: 6-31+g(d,p) optimized geometries

	Conformer	6-31g+(d,p) characterization	6-311+g(2d,p) energy (hartrees)	6-31g+(d,p) thermal correction (hartrees)	6-311+g(2d,p) corrected energy (hartrees)
2aa	Axial chair	Transition state	−648.582951	0.205709	Transition state
2bb	Equatorial chair	Transition state	−648.582348	0.205934	Transition state
2a	Asymmetrical axial chair	Minimum	−648.583774	0.206272	−648.377502
2a	Asymmetrical axial chair	Minimum	−648.583774	0.206272	−648.377502
2b	Asymmetrical equatorial chair	Minimum	−648.583217	0.206279	−648.376938
2b	Asymmetrical equatorial chair	Minimum	−648.583217	0.206279	−648.376938
2c	Syn-twist	Minimum	−648.580968	0.205829	−648.375139
2c	Syn-twist	Minimum	−648.580968	0.205829	−648.375139
2d	Anti-twist	Minimum	−648.580688	0.205821	−648.374867
2d	Anti-twist	Minimum	−648.580688	0.205821	−648.374867
2e	Axial boat	Not critical point			Not critical point
2e	Axial boat	Not critical point			Not critical point
2f	Equatorial boat	Not critical point			Not critical point
2f	Equatorial boat	Not critical point			Not critical point

Table 12. Conformational analysis and calculation of distribution coefficients: 6-311+g(2d,p)//6-31+g(d,p) results

	Conformer	Energy (hartrees)	Energy (J)	Boltzmann distribution (d_i) $[e^{-(E_i-E_0)}/kT]$	Distribution coefficient (c_i) $[e^{-(E_i-E_0)/kT}/\sum_i e^{-(E_i-E_0)/kT}]$
2aa	Axial chair		Transition state		Transition state
2bb	Equatorial chair	Transition state			Transition state
2a	Axial chair	−648.377502	−2.826764E-15	1.000000E+00	0.295335
2a	Axial chair	−648.377502	−2.826764E-15	1.000000E+00	0.295335
2b	Equatorial chair	−648.376938	−2.826761E-15	5.498436E-01	0.162388
2b	Equatorial chair	−648.376938	−2.826761E-15	5.498436E-01	0.162388
2c	Syn-twist	−648.375139	−2.826754E-15	8.181673E-02	0.024163
2c	Syn-twist	−648.375139	−2.826754E-15	8.181673E-02	0.024163
2d	Anti-twist	−648.374867	−2.826752E-15	6.133200E-02	0.018113
2d	Anti-twist	−648.374867	−2.826752E-15	6.133200E-02	0.018113
2e	Axial boat	Not critical point			Not critical point
2e	Axial boat	Not critical point			Not critical point
2f	Equatorial boat	Not critical point			Not critical point
2f	Equatorial boat	Not critical point			Not critical point

Table 13. Calculated magnetic shielding tensors for methylene protons on six-membered ring: 6-31+g(d,p) geometries

Conformer	Distribution coefficient	Calculated magnetic shielding tensors for ring methylene proton				Weighted magnetic shielding tensors for ring methylene proton			
		24	25	26	27	24	25	26	27
2aa	Transition state	28.8256	29.2355	29.2353	28.8252				
2bb	Transition state	29.2482	28.8347	28.8347	29.2482				
2a	0.288232	28.7772	29.1913	29.2614	28.8828	8.2945	8.4139	8.4341	8.3249
2a	0.288232	28.8828	29.2614	29.1913	28.7772	8.3249	8.4341	8.4139	8.2945
2b	0.155166	29.2664	28.9049	28.8092	29.2143	4.5411	4.4851	4.4702	4.5331
2b	0.155166	29.2143	28.8092	28.9049	29.2664	4.5331	4.4702	4.4851	4.5411
2c	0.023357	29.1016	29.2934	29.1748	29.3558	0.6797	0.6842	0.6814	0.6857
2c	0.023357	29.3558	29.1748	29.2934	29.1016	0.6857	0.6814	0.6842	0.6797
2d	0.033245	29.1412	29.3345	29.1291	29.2957	0.9688	0.9752	0.9684	0.9739
2d	0.033245	29.2957	29.1291	29.3345	29.1412	0.9739	0.9684	0.9752	0.9688
2e	Not critical point								
2e	Not critical point								
2f	Not critical point								
2f	Not critical point								
			Weighted average			29.0018	29.1125	29.1125	29.0018
			Calculated average difference			0.1107 ppm			
			Experimental difference			0.1000 ppm			

Table 14. Calculated magnetic shielding tensors for protons on methyl substituents: 6-31+g(d,p) geometries

Conformer	Distribution coefficient	Calculated magnetic shielding tensors for methyl group 1				Calculated magnetic shielding tensors for methyl group 2				Weighted averages	
		17	18	19	Average	21	22	23	Average	Methyl 1	Methyl 2
2aa	Transition state	31.7255	31.7255	31.9340	31.7950	30.3046	31.7252	31.7252	31.2517		
2bb	Transition state	31.7249	31.7249	30.2791	31.2430	31.9650	31.7380	31.7380	31.8137		
2a	0.288232	31.7209	31.7203	31.9228	31.7880	30.3013	31.7161	31.7234	31.2469	9.1623	9.0064
2a	0.288232	31.7203	31.7209	31.9228	31.7880	30.3013	31.7234	31.7161	31.2469	9.1623	9.0064
2b	0.155166	31.7203	31.7170	30.2748	31.2374	31.9584	31.7314	31.7346	31.8081	4.8470	4.9355
2b	0.155166	31.7170	31.7203	30.2748	31.2374	31.9584	31.7346	31.7314	31.8081	4.8470	4.9355
2c	0.023357	31.7135	31.7767	31.1071	31.5324	31.0788	31.7290	31.7783	31.5287	0.7365	0.7364
2c	0.023357	31.7767	31.7135	31.1071	31.5324	31.0788	31.7783	31.7290	31.5287	0.7365	0.7364
2d	0.033245	31.7321	31.7597	31.0429	31.5116	31.1483	31.7074	31.7869	31.5475	1.0476	1.0488
2d	0.033245	31.7597	31.7321	31.0429	31.5116	31.1483	31.7869	31.7074	31.5475	1.0476	1.0488
2e	Not critical point										
2e	Not critical point										
2f	Not critical point										
2f	Not critical point										
						Weighted average				31.5868	31.4542
						Calculated average difference				0.1326 ppm	
						Experimental difference				0.1000 ppm	

Table 15. Calculated magnetic shielding tensors for methylene protons on six-membered ring: 6-31+g(d,p) geometries and 6-311+g(2d,p) energies

Conformer	Distribution coefficient	Calculated magnetic shielding tensors for ring methylene proton				Weighted magnetic shielding tensors for ring methylene proton			
		24	25	26	27	24	25	26	27
2aa	Transition state	28.8256	29.2355	29.2353	28.8252				
2bb	Transition state	29.2482	28.8347	28.8347	29.2482				
2a	0.295335	28.7772	29.1913	29.2614	28.8828	8.4989	8.6212	8.6419	8.5301
2a	0.295335	28.8828	29.2614	29.1913	28.7772	8.5301	8.6419	8.6212	8.4989
2b	0.162388	29.2664	28.9049	28.8092	29.2143	4.7525	4.6938	4.6783	4.7441
2b	0.162388	29.2143	28.8092	28.9049	29.2664	4.7441	4.6783	4.6938	4.7525
2c	0.024163	29.1016	29.2934	29.1748	29.3558	0.7032	0.7078	0.7050	0.7093
2c	0.024163	29.3558	29.1748	29.2934	29.1016	0.7093	0.7050	0.7078	0.7032
2d	0.018113	29.1412	29.3345	29.1291	29.2957	0.5278	0.5314	0.5276	0.5306
2d	0.018113	29.2957	29.1291	29.3345	29.1412	0.5306	0.5276	0.5314	0.5278
2e	Not critical point								
2e	Not critical point								
2f	Not critical point								
2f	Not critical point								
			Weighted average			28.9966	29.1070	29.1070	28.9966
			Calculated average difference			0.1104 ppm			
			Experimental difference			0.1000 ppm			

Table 16. Calculated magnetic shielding tensors for protons on methyl substituents: 6-31+g(d,p) geometries and 6-311+g(2d,p) energies

Conformer	Distribution coefficient	Calculated magnetic shielding tensors for methyl group 1				Calculated magnetic shielding tensors for methyl group 2				Weighted averages	
		17	18	19	Average	21	22	23	Average	Methyl 1	Methyl 2
2aa	Transition state	31.7255	31.7255	31.9340	31.7950	30.3046	31.7252	31.7252	31.2517		
2bb	Transition state	31.7249	31.7249	30.2791	31.2430	31.9650	31.7380	31.7380	31.8137		
2a	0.295335	31.7209	31.7203	31.9228	31.7880	30.3013	31.7161	31.7234	31.2469	9.3881	9.2283
2a	0.295335	31.7203	31.7209	31.9228	31.7880	30.3013	31.7234	31.7161	31.2469	9.3881	9.2283
2b	0.162388	31.7203	31.7170	30.2748	31.2374	31.9584	31.7314	31.7346	31.8081	5.0726	5.1653
2b	0.162388	31.7170	31.7203	30.2748	31.2374	31.9584	31.7346	31.7314	31.8081	5.0726	5.1653
2c	0.024163	31.7135	31.7767	31.1071	31.5324	31.0788	31.7290	31.7783	31.5287	0.7619	0.7618
2c	0.024163	31.7767	31.7135	31.1071	31.5324	31.0788	31.7783	31.7290	31.5287	0.7619	0.7618
2d	0.018113	31.7321	31.7597	31.0429	31.5116	31.1483	31.7074	31.7869	31.5475	0.5708	0.5714
2d	0.018113	31.7597	31.7321	31.0429	31.5116	31.1483	31.7869	31.7074	31.5475	0.5708	0.5714
2e	Not critical point										
2e	Not critical point										
2f	Not critical point										
2f	Not critical point										
						Weighted average				31.5868	31.4537
						Calculated average difference				0.1331 ppm	
						Experimental difference				0.1000 ppm	

structures identified by the 6-31+g(d,p) optimizations (**2c** and **2d**) were found to be significant contributors to the spectrum.

The agreement between ^{1}H-NMR chemical shifts calculated at the 6-311+g(2d,p)//6-31+g(d,p) level of theory and observed values is consistent with the suggestion that intramolecular chemical shift differences can be calculated to a higher degree of accuracy than chemical shifts calculated relative to a standard. It also is hypothesized that differences in chemical shifts between isomers calculated using identical levels of theory and basis sets will exhibit similar improvements to accuracy. Future work will include tests of these hypotheses for a large sample of structures chosen to include a range of electronic environments and previously found to produce large errors in relative chemical shift calculations.

ACKNOWLEDGMENT

This research was supported in part by NIH/NIDR Grant Nos. DE08450 and DE09696.

REFERENCES

1 Stansbury, J.W. Free radical ring-opening polymerization of unsaturated, asymmetric spiro orthocarbonates. Ph.D. thesis, University of Maryland, College Park, 1988

2 AMPAC , version 6.0, 1998, Semichem, Shawnee Mission, KS

3 Iratçabal, P., and Liotard, D. Topological aspects of conformational coupling in 8,8-dimethyl-1, 4-dihetero-spiro [4.5] decanes: A molecular mechanics study. *J. Am. Chem. Soc.* 1988, **110,** 4919–4926

4 Iratçabal, P., and Liotard, D. Conformational dynamics of 9,9-dimethyl-1.5-dihetero-spiro[5.5] undecanes by molecular mechanics calculations: A three-dimensional topological approach. *J. Comput. Chem.* 1986, **9,** 482–493

5 Cheeseman, J.R., Trucks, G.W., Keith, T.A., and Frisch, M.J. A comparison of models for calculating nuclear magnetic resonance shielding tensors. *J. Chem. Phys.* 1996, **104,** 5497–5509

6 Gauss, J. Effects of electron correlation in the calculation of nuclear magnetic resonance chemical shifts. *J. Chem. Phys.* 1993, **99,** 3629–3643

7 Wolinski, K., Hinton, J.F., and Pulay, P. Efficient implementation of the gauge-independent atomic orbital method for NMR chemical shift calculations. *J. Am. Chem. Soc.* 1990, **112,** 8251–8260

8 Keith, T.A., and Bader, R.F.W. Calculation of magnetic response properties using atoms in molecules. *Chem. Phys. Lett.* 1992, **194,** 1–8

9 Keith, T.A., and Bader, R.F.W. Calculation of magnetic response properties using a continuous set of gauge transformations. *Chem. Phys. Lett.* 1993, **210,** 223–231

10 Ditchfield, R. Self-consistent perturbation theory of diamagnetism: A gauge-invariant LCAO method for N.M.R. chemical shifts. *Mol. Phys.* 1974, **27,** 789–807

11 Vaara, J., Ruud, K., Vahtras, O., Ågren, H., and Jokisaari, J. Quadratic response calculations of the electronic spin-orbit contribution to nuclear shielding tensors. *J. Chem. Phys.* 1998, **109,** 1212–1222

12 Gaussian 94, revision D.1, 1993, M.J. Frisch, G.W. Trucks, H.B. Schlegel, P.M.W. Gill, B.G. Johnson, M.A. Robb, J.R. Cheeseman, T.A. Keith, G.A. Petersson, J.A. Montgomery, K. Raghavachari, M.A. Al-Laham, V.G. Zakrzewski, J.V. Ortiz, J.B. Foresnam, J. Cioslowski, B.B. Stefanov, A. Nanayakkara, M. Challacombe, C.Y. Peng, P.Y. Ayala, W. Chen, M.W. Womng, J.L. Andres, E.S. Replogle, R. Gomperts, R.L. Martin, D.J. Fox, J.S. Binkley, D.J. Defrees, J. Baker, J.P. Stewart, M. Head-Gordon, C. Gonzalez, and J.A. Pople, Gaussian, Inc., Pittsburgh, PA